Available online at www.sciencedirect.com
SCIENCE DIRECT®
Polymer 44 (2003) 6901–6911
polymer
www.elsevier.com/locate/polymer

Chemorheology of cyanate ester—organically layered silicate nanocomposites

Sabyasachi Ganguli[a], Derrick Dean[a,*], Kelvin Jordan[b], Gary Price[c], Richard Vaia[d]

[a]*Tuskegee-Center for Advanced Materials, Tuskegee University, 101 Chappie James Center, Tuskegee, AL 36088, USA*
[b]*Raytheon Electronic Systems, Tuscon, AZ, USA*
[c]*University of Dayton Research Institute, Dayton, OH, USA*
[d]*Air Force Research Laboratory, Materials and Manufacturing Directorate, WPAFB, Dayton, OH, USA*

Received 11 March 2003; received in revised form 30 July 2003; accepted 3 August 2003

Abstract

The effect of nanoparticle addition on the flow and curing behavior of a phenolic triazine cyanate ester resin system has been studied using chemorheological, thermal and spectroscopic techniques. While the neat system exhibited Newtonian flow, the nanodispersed prepolymer exhibited pseudoplastic flow behavior, typical of polymeric fluids such as gels and pastes. Evolution of the morphology during curing has been found to be dependent on the rate of intergallery diffusion of the prepolymer and subsequent gelation and vitrification, as well as the intra and extragallery cure kinetics. Curing reactions of the cyanate ester nanocomposite system consisting of a di-functional phenol, a halogen cyanate and organically layered silicates were studied. Gel times were measured as a function of temperature by time sweeps on a controlled stress rheometer. Gelation and vitrification times and activation energies for the nanocomposite systems were lower than that of the neat resins, indicating a catalytic effect of the clays on the curing reaction. Curing kinetics experiments performed on DSC and FTIR confirmed this phenomenon. Based on above experiments, time–temperature-transformation diagrams for the different systems were constructed.

Keywords: Chemorheology; Polymer–clay nanocomposites; Silicate nanocomposites

1. Introduction

Pioneering advances at Toyota research [1] during the early 1990s has stimulated the development of various polymer/organoclay nanocomposites with attractive property profiles such as improved stiffness combined with elevated dimensional stability, barrier resistance, improved thermal stability and inherent flame retardency.

Numerous methods to prepare polymer–clay nanocomposites have recently been developed by several groups [2–6]. One of the goals has been to understand the parameters required for controlling dispersion of the clay within the polymer. Two types of dispersions are typically achieved: intercalated in which the polymer chains are located between the clay layers, and exfoliated, in which the polymer fully delaminates the clay layers. Pinnavaia et al. have achieved exfoliated morphologies using epoxy resins [6]. The ability to achieve an exfoliated morphology is presumably due primarily to the relatively high polarity of these systems, which promotes diffusion into the clay galleries. Subsequent to diffusion into the interlayer, it was suggested that the maximum layer expansion is obtained when intragallery polymerization rates exceed that in the extragallery regions allowing exfoliation to occur before gelation. It was also shown that the acidity of the alkylammonium ions catalyzes homopolymerization of DGEBA epoxy resins.

Several studies have dealt with the structure property relationships of thermoplastic polymer clay nanocomposites, but few have studied the rheology of these multiphase systems [7–10]. This is extremely important, particularly for thermoset systems, because the ability to process thermoset based nanocomposites depends on several factors such as the composition of the thermoset (e.g. prepolymer, curing agent, catalyst nanoparticle, etc.) and its effect on the cross-linking reaction, since the extent of cross-linking determines the gel point of the system and ultimately the

* Corresponding author. Tel.: +1-334-724-4247; fax: +1-334-727-4224.
E-mail address: deand@tusk.edu (D. Dean).

0032-3861/$ - see front matter © 2003 Published by Elsevier Ltd.
doi:10.1016/j.polymer.2003.08.031

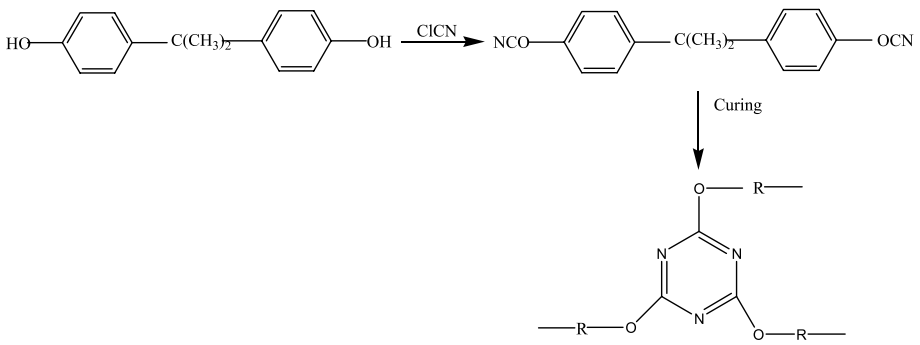

Fig. 1. Network formation of triazines from cyanate esters where R = $C_{15}H_{14}$.

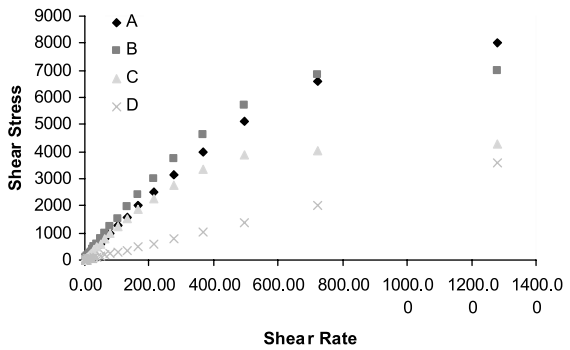

Fig. 2. Room temperature flow behavior of the neat and nanodispersed systems, A = 5%, B = 2.5%, C = 1% and D = neat cyanate ester resin.

final morphology (i.e. exfoliated versus intercalated). Therefore, understanding and control of the effect of the clay surface modifiers on the kinetics of the curing is critical [11,12].

Cyanate ester resins are among the most important engineering thermosetting polymers and have received attention because of their outstanding physical properties such as low water absorptivity and outgassing and excellent mechanical properties, dimensional and thermal stability and flame resistance [13–16]. In addition to their excellent thermal stability, cyanate ester resins are relatively easy to process [15]. They have been used for various applications and can be processed in a manner similar to epoxies. Since the curing of cyanate esters occurs through addition polymerization of cyanate rings forming triazine moieties, no volatiles are generated [14a]. A typical reaction mechanism for polycyanurate formation, as shown in Fig. 1, involves reaction of a difunctional phenol with a cyanogen halide (typically cyanogen chloride in

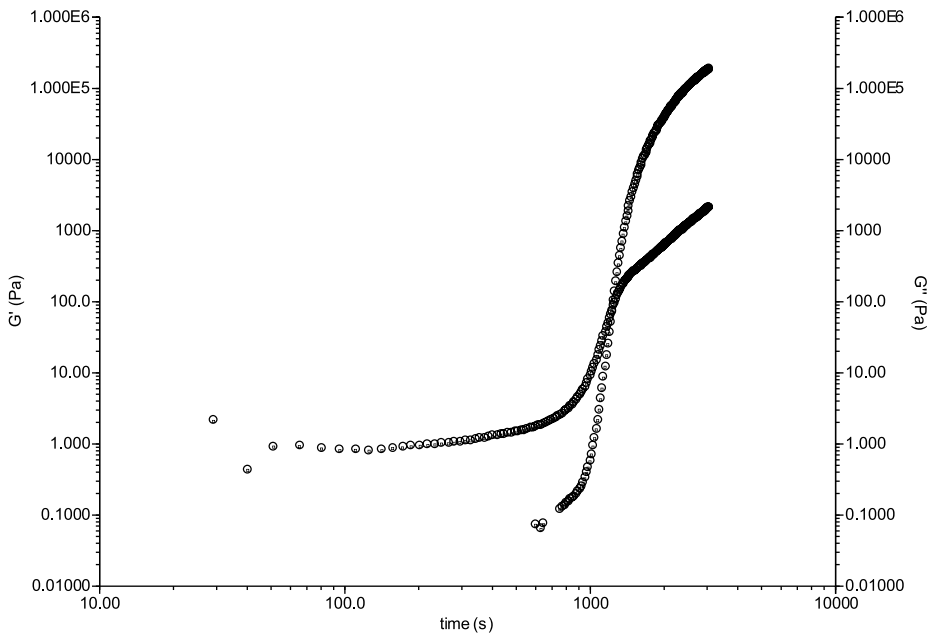

Fig. 3. Evolution of storage and loss moduli over time at 188 °C for the 5% nanocomposite.

Table 1
Gel times for neat and nanocomposites of cyanate ester

Specimen	Temperature (°C)	Gel times (min)
Neat	80	271
	100	233
	120	177
	135	93
	150	42
	170	39
	190	31
1% Nanocomposite	80	232
	100	201
	120	126
	135	74
	150	39
	170	27
	190	24
2.5% Nanocomposite	80	178
	100	142
	120	117
	135	63
	150	52
	170	29
	190	22
5% Nanocomposite	80	174
	100	138
	120	112
	135	59
	150	48
	170	27
	190	20

commercial preparations) to yield an intermediate oligomer (MW ~ 2K) [14a]. Cross-links are formed by the triazine rings. It is noted that several potential side reactions, such as substitution effects, intramolecular cyclization and diffusional hindrance, could lead to 'flaws' in the network formation [16]. In a previous study [13] we reported on the synthesis and mechanical properties of cyanate ester–clay nanocomposites. Small additions of modified silicates resulted in a 90 °C increase in T_g and a 30% improvement in the modulus and strength, respectively. In this paper, we report on the chemorheological behavior of these nanocomposite systems. The effect of the clays on the development of cure (gelation, vitrification) and the morphology evolution was studied by rheology and X-ray diffraction. The data was used to calculate time–temperature-transformation (TTT) diagrams for the neat cyanate ester and nanocomposite systems. This diagram is a useful tool for the design of cyanate ester resin curing cycles, because it records the effects of the nanoparticles on the phenomenological changes associated with curing, such as gelation and vitrification as a function of time and/or temperature.

Table 2
Activation energy obtained from DSC and rheology

Specimens	DSC (kJ/mol)	Rheology (kJ/mol)
Neat resin	46	37
1% Nanocomposite	44	30
2.5% Nanocomposite	24	24
5% Nanocomposite	16	15

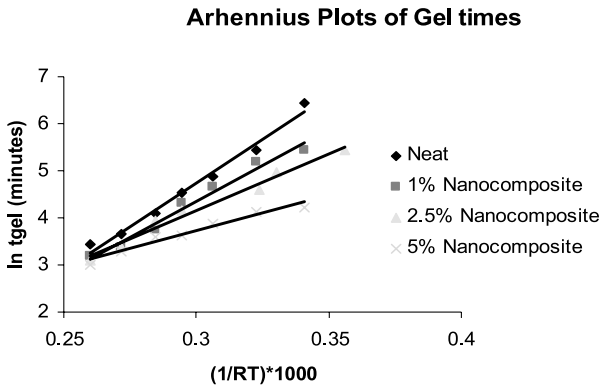

Fig. 4. Arhennius plots of gel times from rheology data.

2. Experimental

A phenolic-based cyanate ester resin, RS9RTM, was kindly supplied by YLA Inc. It is a low viscosity resin transfer moldable version of the cyanate ester resin. It contains a proprietary formulation of cobaltacetylacetonate as the catalyst. Cloisite 30B modified montmorillonite was also kindly by Southern Clay Products. The Cyanate Ester resin was placed in a ceramic crucible, which was maintained at a temperature of 60–65 °C using a hot plate. A high-shear mixing blade was placed into the resin and stirred at 52 rad/s (500 rpm). Cloisite 30B was slowly added (1, 2.5 and 5 wt%) and mixed for 15 min. The mixture was then sonicated using an ultrasonic probe for 2 min. The high shear mixing did not completely disperse the clay, thus the ultrasonic probe was used to improve the dispersion of the clay in the polymer matrix. Shearing with the ultrasonic probe for longer than 2 min resulted in initiation of curing. The cure schedule was: heat to 110 °C over 120 min under vacuum, then ramp to 188 °C at 5 °C/min and hold for 120 min; then cool to 30 °C over 60 min.

Thermogravimetric analysis (TGA) was performed using a TA Instruments TGA 2950 at 10 °C/min in air. The glass transition temperature ($T_{g\infty}$) of the fully cured samples was obtained using a TA Instruments DMA 2980 in the single cantilever mode (strain amplitude of 10 μm, oscillatory frequency of 1 Hz, and heating rate of 3 °C/min). The samples were rectangular and the dimensions were 30 mm × 6 mm × 3 mm.

The dispersion quality was measured using wide angle X-ray scattering (WAXS) measurements performed on a

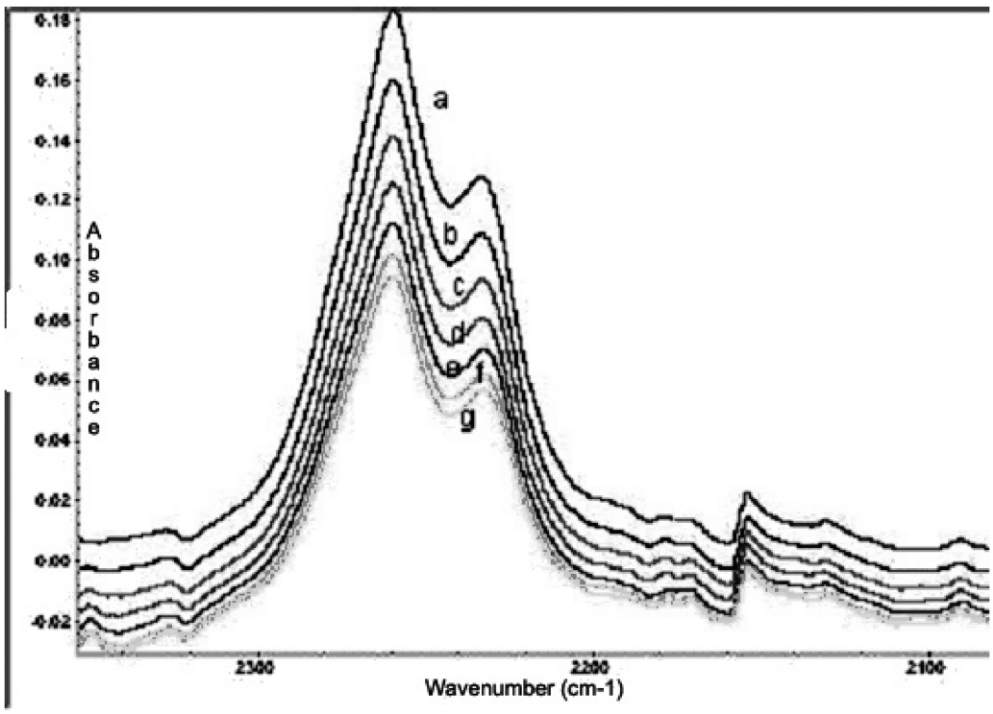

Fig. 5. Isothermal IR interferograms of neat Cyanate ester at 188 °C, $a = 0$ min, $b = 5$ min, $c = 10$ min, $d = 15$ min, $e = 20$ min, $f = 25$ min, and $g = 30$ min.

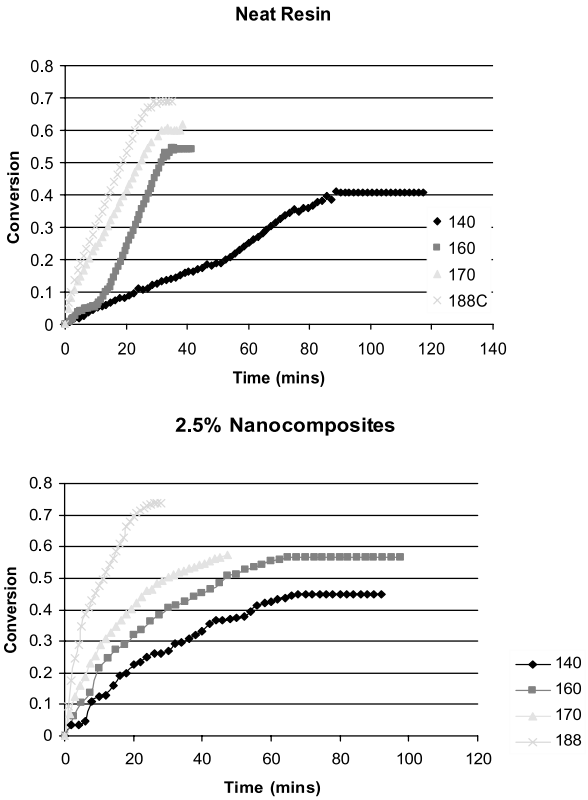

Fig. 6. Evolution of conversion (by FTIR) versus time and temperature for neat cyanate ester and 2.5% nanocomposite.

Bruker D8 Discover system with Eulerian 1/4 cradle, GADDS software and Cu Kα radiation ((40 kV, 40 mA). The samples (thickness = 0.14 mm) were run in transmission with the detector (sample to detector distance of 15 cm) centered at $2\theta = 22°$. Patterns, collected for 20 min, were radially integrated (60°). Additional scans were conducted on a Rigaku RU200 rotating anode generator equipped with a Statton camera. Nickel filtered Cu Kα radiation was used at an accelerating voltage of 50 kV/170 mA. The data was collected on phosphor image plates and digitized using a Molecular Dynamics scanner.

Rheological experiments were conducted on a controlled stress rheometer (AR 2000, TA Instruments Inc, Delaware) in parallel plate mode. Isothermal time sweeps and steady state stress ramps (0–65,190 Pa) were conducted. Steady state stress ramp tests were conducted at 40 °C.

A differential scanning calorimeter (TA Instruments DSC 2010) was used to determine T_{g0}, (glass transition behavior of the prepolymer or glass transition temperature corresponding to zero conversion). It was also used for determining curing kinetics for the neat and nanodispersed systems based on ASTM E698. The ASTM approach uses the variable program rate method of Ozawa [17], which requires three or more scan rates. Scan rates of 5, 10, 20 and 30 °C/min were used in this study. This method also assumes Arrhenius behavior and first order reaction kinetics [18,19].

FTIR measurements were performed with a Nicolet spectrometer, using a Specac Golden Gate Attenuated Total

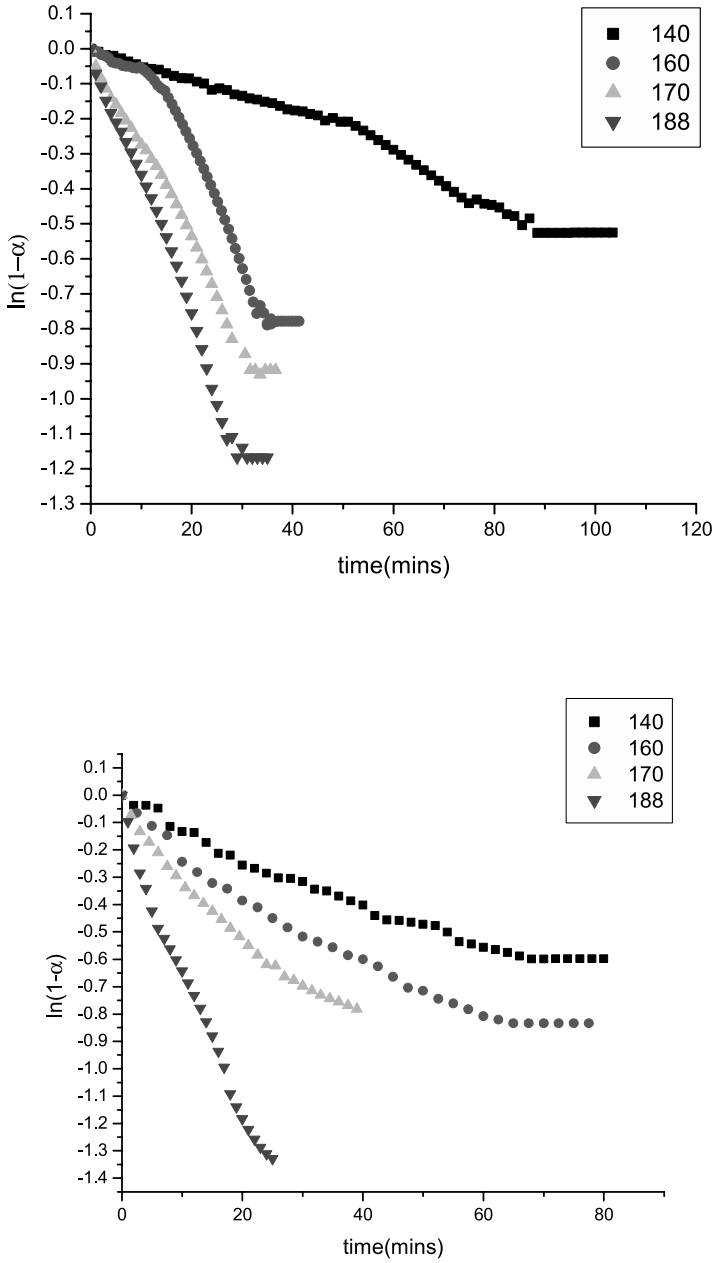

Fig. 7. Kinetic plot of ln(1 − α) versus ln(time), time from FTIR data.

Reflectance Accessory (ATR), using 64 scans with a 4 cm^{-1} resolution step. Sample was placed on the ATR diamond cell, and the temperature was controlled by a Eurotherm 2216E controller. FTIR scans were acquired at 2 min intervals.

3. Results and discussion

3.1. Flow behavior

Fig. 2 shows the room temperature flow behavior of the neat prepolymer and the nanodispersed systems. As expected, the neat prepolymer exhibits Newtonian flow, while the nanodispersed systems exhibit pseudoplastic flow, which is more typical of polymeric dispersed fluids such as gels and pastes [20]. The neat cyanate esters are uncured and hence still a low molecular weight prepolymer, thus the observed flow behavior may be due to polymer–clay interactions as well as resistance to flow brought about by the presence of the relatively large, anisotropic silicate layers. Evaluation of the shear stress, τ, reveals that the viscosity, η, of the prepolymer increases when the clay is added, but the increase is only a factor of ca. 2.5 for the

Table 3
Glass transition temperatures for the uncured resin (T_{g0}) and the fully cured neat resin and its nanocomposites (T_α)

	T_{g0}	T_α
Neat	−14	305
1% Nanocomposite	−5	329
2.5% Nanocomposite	−5	378
5% Nanocomposite	−5	390

highest clay loading. The relatively small increase in viscosity upon clay addition (500–200 P) suggests that processing of these nanocomposites is feasible.

3.2. Cure behavior and morphology development

Previous studies conducted on the morphological development of the system indicates intercalation of the prepolymer into the clay galleries, resulting in an intergallery expansion from 17.38 Å ($2\theta = 4.9°$) for Cloisite 30B [13,21] to 35 Å ($2\theta = 2.5°$). Curing the prepolymer results in a slight gallery height increase to 40 Å ($2\theta = 2.2°$) indicative of a small degree of mass transfer into the galleries as the curing proceeds. Presumably, the OLS surfaces catalyze the curing process, leading to rapid gelation, which retards diffusion of the prepolymer into the galleries and inhibits extensive layer separation [3]. In a recent study on an epoxy/clay system, Ober et al. suggest that exfoliation is obtained when the rate of extragallery polymerization is slower than the intragallery polymerization [9]. When this occurs, the faster curing and stiffening of the intragallery polymer leads to compression of the extragallery layers. We note that it is very difficult to delineate the true mechanism without a high-resolution probe that can preferentially study the intragallery reactions versus those that occur in the extragallery regions. Nevertheless, the nanoscale reactions are believed to significantly affect the morphology development. Synthesis of the nanocomposites involves polymerizing the cyanurate in the presence of the clays. The formation of the polycyanurate network occurs through polycyclotrimerization of the cyanate ester groups via a step growth process (see Fig. 1) [13,14]. The chemical and physical structure of the network is closely related to the formation process, which in turn may be affected by the clays. Therefore understanding issues such as the effect of the clays on the gel points and the kinetics of the cure is essential to developing the processing parameters. The gel times were experimentally determined by conducting isothermal time sweeps on a rheometer at 80, 90, 100, 120, 135, 149, 163 and 188 °C, respectively. The gel times were taken as the cross-over point between the storage and loss moduli (a representative curve for the resin systems is shown Fig. 3) and represent the point at which the material transforms from a liquid to a rubber.

Table 4
Vitrification times for neat and nanocomposites of cyanate ester

Specimen	Temperature (°C)	Vitrification times (min)
Neat	80	410
	100	373
	120	252
	135	135
	150	71
	170	62
	190	50
1% Nanocomposite	80	372
	100	325
	120	201
	135	118
	150	57
	170	46
	190	32
2.5% Nanocomposite	80	282
	100	228
	120	163
	135	77
	150	37
	170	26
	190	18
5% Nanocomposite	80	278
	100	227
	120	149
	135	73
	150	40
	170	21
	190	15

The gel points for the neat resin and nanodispersed systems are shown in Table 1. While it is difficult to differentiate the contributions of intra and extragallery polymerization to the gelation behavior, it is assumed that the decrease in gel times as a function of clay loadings is due to catalyzation by the modified clay surfaces [3,9,13]. This is corroborated by the activation energies of gelation (Table 2), which decrease with increased clay loadings. The reduction in activation energies with increased clay loadings suggests that the clay catalyzes the curing reaction. The activation energies have been calculated from the time sweep data (assuming Arhennius behavior) by taking the slope of the $\ln t_{gel}$ versus $1/(RT)$ plots, which are shown in Fig. 4. The time window for dispersing the clay into the system decreases upon clay addition. Furthermore, as the system gels and vitrifies, the T_g evolves, eventually surpassing the cure temperature [22,23]. At this point, further clay expansion would be highly unlikely. Therefore, any structure obtained at this point (intercalated or exfoliated) would be essentially 'locked in' by the cross-linked structure. Correlation of gel times with the morphological data suggests that, depending on the cure temperature, the intercalated morphology develops at a relatively early stage of the cure process (e.g. α_{gel} at 190 °C is 30 min, while total cure time is 4 h). Assuming the proper conditions for reproducibly achieving an exfoliated

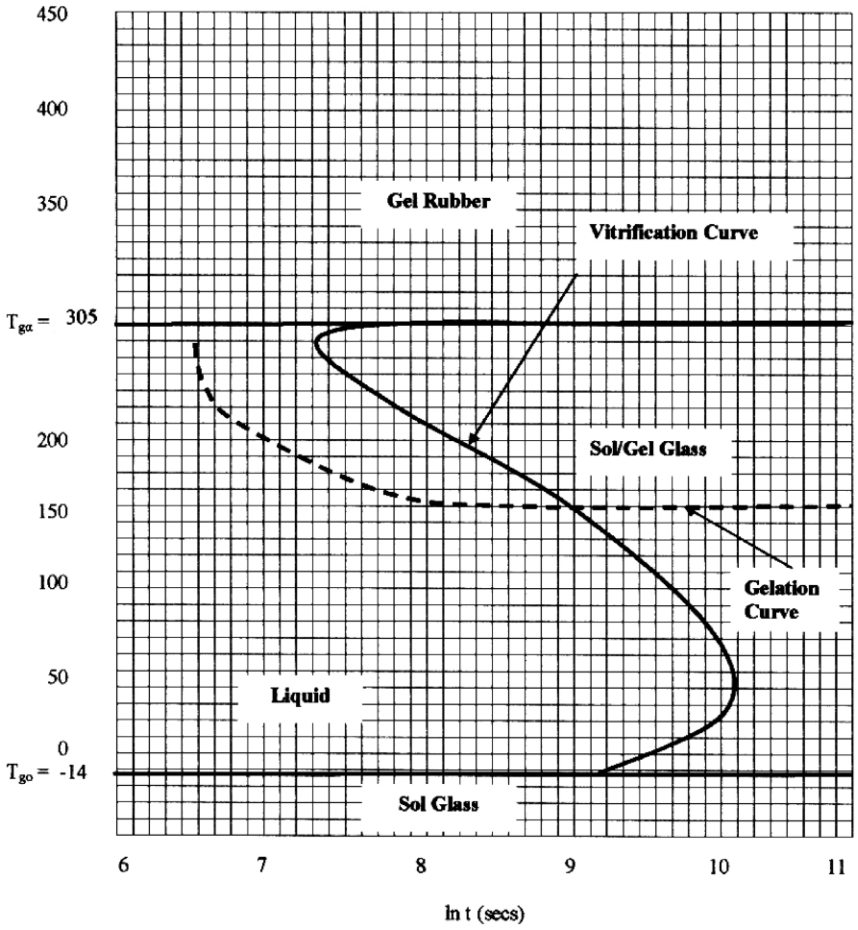

Fig. 8. TTT plot for neat cyanate ester.

morphology can be determined, the rheological experiment could be a cost effective tool for inferring the morphology.

In addition to knowing the gel points of the curing system, knowledge of the degree of conversion of the thermosetting reaction is also critical to development of a complete picture of the curing process. The extent of cure at the gel point was determined by FTIR. The FTIR method [14] involved monitoring the decrease in the absorbance of the νCN triple bond, which has a characteristic absorbance peak between 2200 and 2400 cm^{-1}. The decrease of this peak as a function of cure time for the neat resin is shown in Fig. 5 and is considered representative of the all the samples. A ratio of the peak area to that of an internal reference band is taken. The internal reference band is attributed to the aliphatic C–H band in the 2900–2850 cm^{-1} region. This ratio is then used in the following equation to calculate the degree of conversion, α, where

$$\alpha = \frac{\dfrac{A_t^{CN}}{A_t^{C-H}}}{\dfrac{A_{t=0}^{CN}}{A_{t=0}^{C-H}}}$$

where A_t^{CN} and $A_{t=0}^{CN}$ are area under the νCN vibration band at time t and $t = 0$, respectively, A_t^{C-H} and $A_{t=0}^{C-H}$ are the areas under the aromatic C–H band at time t and $t = 0$, respectively [22].

Fig. 6 shows the evolution of conversion versus time and temperature of isothermal curing for the neat resin and the 2.5% clay system. The conversion increases with time under given isothermal conditions and with the temperature of isothermal cure. Correlation of the degree of conversions with the gel points indicate that although the nanoparticles reach their gel points faster compared to the neat resin, the overall degree of conversion is about the same. Bartolomeo et al. [22] in a similar study on a different cyanate ester system, obtained conversion levels similar to what we have obtained. Several other studies on cyanate esters have reported αs ranging from 0.6 to 0.7 [14]. The data suggests that the timescale of gelation is shorter for the nanocomposites, while the overall degree of cure is not affected by the clays.

Several kinetic models for the curing of cyanate esters have been developed [14]. In one model, Simon and Gilham have derived a kinetic scheme (equation below) that takes into account both the catalyzed and the uncatalyzed reaction [14]:

$$d\alpha/dt = k_1(1-\alpha)^2 + k_2\alpha(1-\alpha)^2$$

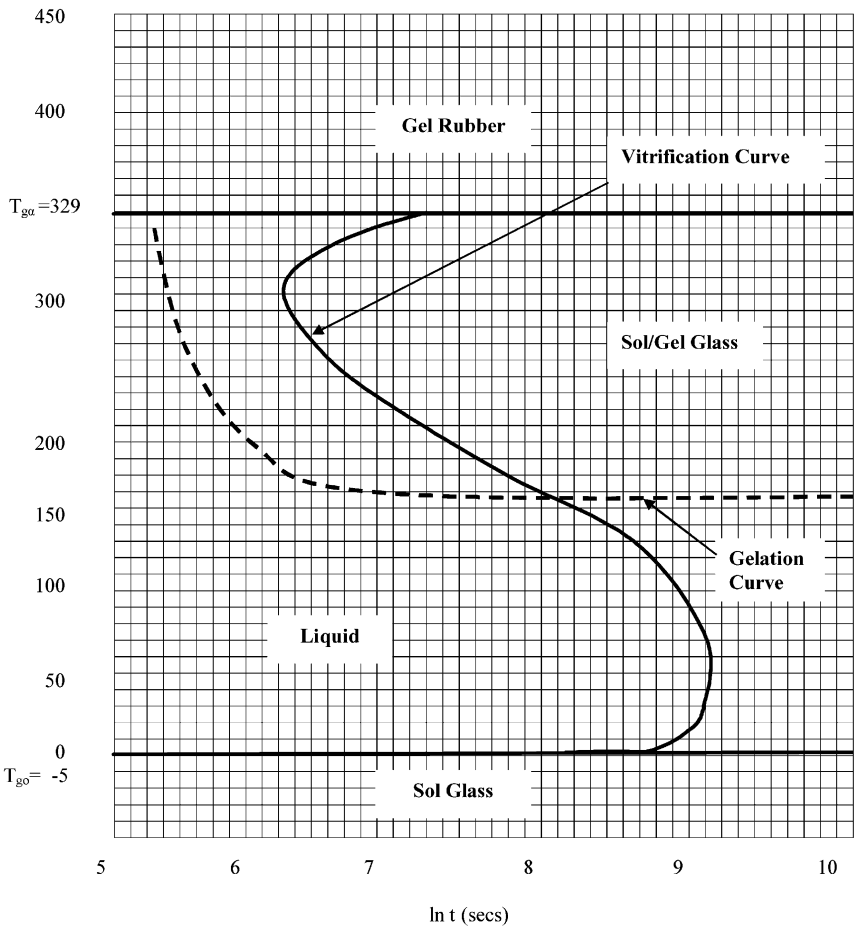

Fig. 9. TTT plot for 1% cyanate ester–clay nanocomposite.

where α is the conversion of the OCN groups and k_1 and k_2 are the rate constants for a second order and a second order autocatalytic reaction. If the temperature or the catalyst concentration is high enough so that the initial phases of the reaction can be neglected [14], the kinetics can be described by a simple nth order kinetic scheme:

$$d\alpha/dt = k(1 - \alpha)^n$$

A replot of the IR data as shown in Fig. 7 indicate that the curing for both systems initially follow first order kinetics as predicted by the equation above, with subsequent onset of diffusional control [14].

ASTM E698 curing kinetics experiment was performed on the DSC. This kinetics approach is based on the variable program rate method of Ozawa [17] which requires three or more experiments at different heating rates, usually between 1 and 10 °C/min. This approach assumes Arhennius behavior and first order kinetics. The method also assumes that the extent of the reaction at the peak exotherm is constant and independent of heating rate.

Activation energies calculated using DSC and rheology are shown in Table 2. The higher clay loadings, 2.5 and 5%, exhibit good agreement between the data obtained from the DSC and rheological methods. Values for the neat resin agree well with values in the literature. For example, Bartolomeo et al. reported E_as ranging from 40 to 50 kJ/mol [22]. Activation energies of 80, 93 and 120 kJ/mol have been reported by Hammerton for different cyanates and reaction conditions [14]. Catalysts were employed in all cases. The observed decrease in E_a as a function of clay loadings suggests that the clays provide a catalytic effect on the curing in addition to that of the formulated catalyst. Elucidation of the particle–polymer interactions is currently underway. Based on the kinetic data, however, the curing mechanisms do not appear to differ from that of a typical catalyzed cyanate ester system.

3.3. Development of TTT diagrams

As stated earlier, the ability to process thermoset based

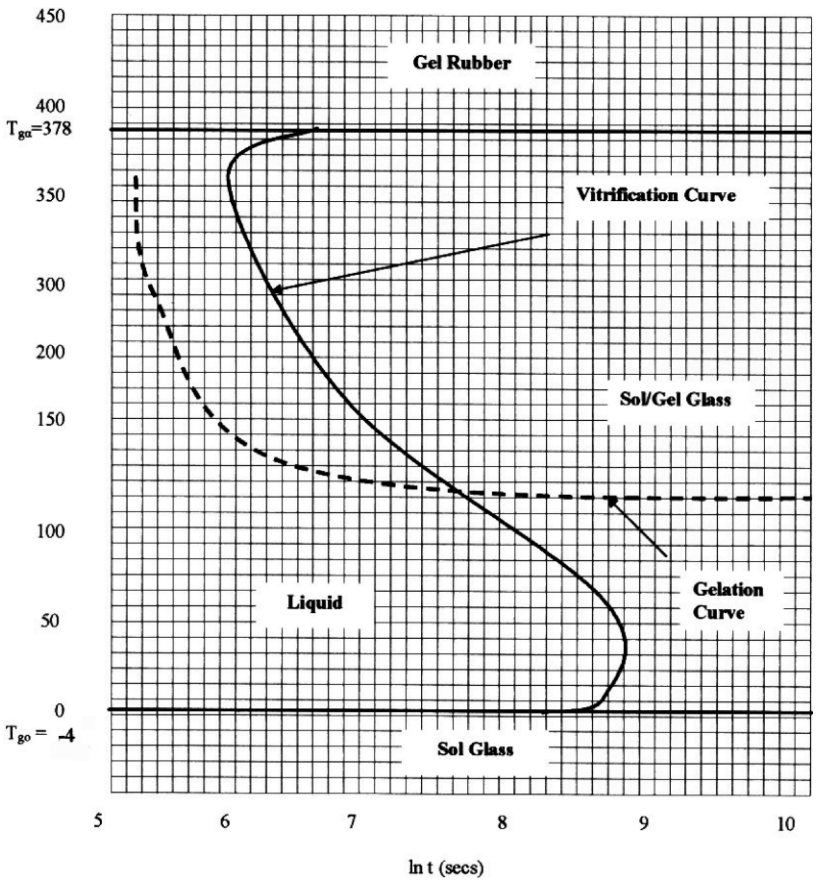

Fig. 10. TTT plot for 2.5% cyanate ester–clay nanocomposite.

nanocomposites will depend on the ability to understand and control the interplay of the thermoset composition and its effect on the state of cure and morphology development. TTT diagrams are a very effective means of displaying the relationship between the pertinent processing parameters (time, temperature) and their effect on the gelation, vitrification and T_g of the cured polymer [23,24]. The main features of such an diagram can be obtained by measuring the times to events that occur during isothermal cure at different temperatures [25]. These events include the onset of phase separation, gelation, vitrification, full cure and devitrification. Gelation corresponds to the incipient formation of an infinite molecular network, which gives rise to long-range elastic behavior in the macroscopic fluid. It occurs at a definite conversion for a given system according to Flory's theory of gelation [26,27]. After gelation the material consists of normally miscible sol and gel fractions, the ratio of the former to the latter decreasing with conversion [25]. Vitrification occurs when the glass transition temperature rises to the isothermal temperature of cure. Devitrification occurs when the T_g decreases through the isothermal temperature as in degradation. The diagram displays the distinct states encountered on cure due to chemical reactions. These states include liquid, sol/gel rubber, ungelled (sol) glass, gelled glass and char. Vitrification times and T_gs were used in conjunction with the data discussed earlier, to develop the TTT diagrams for the neat CE and its nanocomposites. T_gs for the uncured system, T_0 and the cured systems T_∞ were obtained using DSC and DMA, respectively. Vitrification times t_{vitr}, were determined from plots of the storage modulus versus time and correspond to the initial plateau in the curves. Tables 3 and 4, summarize the t_{vitr} and T_g and T_∞ values, respectively. The TTT diagrams are shown in Figs. 8–11.

4. Conclusions

Chemorheological studies have been conducted in order to characterize the effect of organically modified silicates on the cure behavior of cyante ester resin nanocomposites. Flow behavior was observed to change from Newtonian for the neat resin to pseudoplastic for the prepolymer nanocomposites. This behavior is attributed to polymer–clay interactions as well as restriction to flow by the large, anisotropic silicate layers. All of the data (rheology, DSC and FTIR) suggests that the clays have a catalytic effect on curing, as evident by decreases in gel times and activation energies of cure, respectively. Evolution of the morphology indicates an intercalated

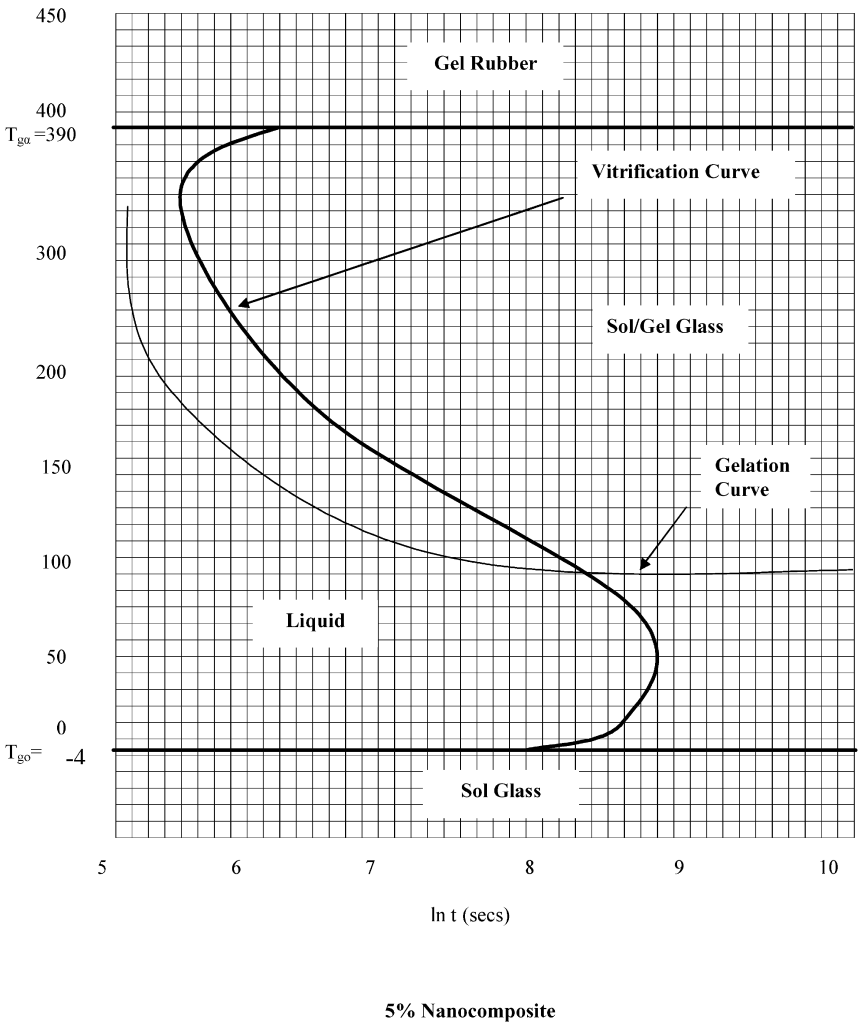

Fig. 11. TTT plot for 5% cyanate ester–clay nanocomposite.

morphology. Enhanced intergallery cure kinetics may be leading to a more rapid vitification which limits mass diffusion into the layers and subsequent exfoliation. It is noted that this resin undergoes rapid curing which also makes the attainment of an exfoliated morphology difficult. Future studies will involve varying the catalyst concentration and evaluating its effect on the chemorheology and an in situ study of the morphology development during cure. In addition, we are currently investigating the chemorheology and morphology development of a model difunctional epoxy nanocomposite in which exfoliated structures are more easily attainable.

Acknowledgements

The authors would like to acknowledge funding from the Air Force Office of Scientific Research and Raytheon Missile systems.

References

[1] Okada A, Kojima Y, Kawasumi M, Fukushima Y, Kurauchi T, Kamigaito O. J Mater Res 1993;8:1179.
[2] Blumstein A. Bull Chim Soc 1961;899.
[3] Le Baron P, Wang Z, Pinnavai T. Appl Clay Sci 1999;15:11–29.
[4] Giannelis EP. Adv Mater 1996;8:29–35.
[5] Kojima Y. J Mater Res 1993;8:1187.
[6] Lan T, Kaviratna PD, Pinnavaia TJ. Epoxy self polymerization in smectite clay. J Phys Chem Solids 1996;57(6–8):1005–10.
[7] Hoffmann B, Dietrich C, Thomann R, Friedrich C, Mulhaupt R. Macromol Rapid Commun 2000;21:57–61.
[8] Halley PJ, Mackay ME. Polym Engng Sci 1996;36:5.
[9] Chen JS, Poliks MD, Ober CK, Zhang Y, Wiesner U, Giannelis E. Polymer 2002;43:4895.
[10] Giannelis EP, Krishnamoorti R, Manias E. Adv Polym Sci 1999;138:107.
[11] Wei X, Gao Z, Pan W-P, Hunter D, Singh A, Vaia R. Chem Mater 2001;13:2979–90.
[12] Tolle TB, Anderson DP. Compos Sci Technol 2002;62:1033–41.
[13] Ganguli S, Dean D, Jordan K, Price G, Vaia R. Polymer 2003;44:1315–9.
[14] (a) Hamerton I. Chemistry and technology of cyanate esters. London: Chapman & Hall; 1994. (b) Lyon RE, Walters R, Gandhi S. DOT/

FAA/AR-02/44. Washington DC: Office of Aviation Research. 20591; 2002. (c) Walters RN. DOT/FAA/AR-02/53. Washington, DC: Office of Aviation Research. 20591; 2002. (d) Ramirez ML, Walters R, Savitski EP, Lyon RE. DOT/FAA/AR-01/32. Washington, DC: Office of Aviation Research. 20591; 2001.

[15] Mackenzie A, Malhotra V, Pearson D, Chow N. Product bulletin ICI. Arizona, USA: Wilton Material Research Center; 1996.

[16] Lin S-C, Pearce EM. High performance thermosets: chemistry, properties, applications. New York: Hanser; 1993.

[17] Ozawa T. Therm Anal 1970;301:2.

[18] Prime RB. Polym Engng Sci 1973;13:365.

[19] Peyser P, Bascom WD. Anal Calorim 1974;3:537.

[20] Cezar Capanescu, Irene Capanescu/Lasco Composites, LP, Florence, KY and Corneliu, Cincu/University of Bucharest, Romania, Paint and Coatings Industry Newsletter Article; May 2002.

[21] Islam M, Dean D, Campbell S. Am Chem Soc Polym Mater: Sci Engng 2001;84.

[22] Bartolomeo P, Chailan JF, Vernet JL. Eur Polym J 2001;37:659–70.

[23] Aronhime M, Gillham J. J Coat Technol 1985;56(718):35–47.

[24] May CA. Chemorheology of thermosetting polymers. American Chemical Society; 1983. ISBN: 0841207941.

[25] Gillham J. Polym Engng Sci 1986;26:20.

[26] Flory PJ. Principles of polymer chemistry. Ithaca, NY: Cornell University Press; 1953.

[27] Gillham J. In: Dawkinns JV, editor. Developments in polymer characterization, vol. 3. London: Applied Science Publishers; 1982. p. 159–227. Chapter 5.